6ICEGE 6th International Conference on Earthquake Geotechnical Engineering
1-4 November 2015
Christchurch. New Zealand

An Effective Stress Analysis considering Permeability of the Ground ~ Liquefaction at a Reclaimed Land in Main and After Shock of the 2011 off the Pacific Coast of Tohoku Earthquake

K. Uemura[1], M. Nobumoto[2], S. Sawada[3], M. Yoshida[4], S. Sato[5],Y. Kageji[6], Y. Tamari[7], J. Hyodo[8], T. Nakama[9], A. Hosoo[10] And K. Ichii[11]

ABSTRACT

In this study, a series of effective stress dynamic analyses considering permeability is done for the areas with and without liquefaction damage at reclaimed land in Urayasu city, Japan. A computer program "FLIP ROSE (Iai et al, 1992, 2011)" with the "Cocktail glass model (Iai et al, 2011)" is used. The parametric study for the permeability of saturated and unsaturated ground is done. As a result, the applicability of the numerical model is confirmed because the simulation of the areas with and without liquefaction damage is successfully agreed with the observation. Especially, the observation of the sand boiling can be explained by the calculated results on the process of the pore water pressure increase. And from the computed results on the timing of sand boiling occurrence, the permeability of the saturated ground after earthquake is estimated to be bigger than the initial permeability.

Introduction

Widespread liquefaction damage occurred in Tokyo bay area by the 2011 off the Pacific coast of Tohoku Earthquake on March 11, 2011. The liquefaction damage was significant because of the fact that the duration of the ground motion is quite long (more than 2 minutes on the main shock) and the aftershock occurred about 30 minute later. The permeability of the ground cannot be ignored in this case.

A series of effective stress dynamic analyses considering the permeability of soils is done for the areas with and without liquefaction damage at reclaimed land in Urayasu city, Japan. A computer program "FLIP ROSE (Iai et al, 1992, 2011)" with the "Cocktail glass model (Iai et al, 2011)" is used.

[1]OYO Corporation, Saitama, Japan, uemura-kazuaki@oyonet.oyo.co.jp
[2]OYO Corporation, Saitama, Japan, nobumoto-minoru@oyonet.oyo.co.jp
[3]OYO Corporation, Saitama, Japan, sawada-shun@oyonet.oyo.co.jp
[4]Penta-Ocean Construction Co., Ltd., Tokyo, Japan, Makoto.Yoshida@mail.penta-ocean.co.jp
[5]Pacific Consultants Co., Ltd., Tokyo, Japan, shigeru.satou@tk.pacific.co.jp
[6]Pacific Consultants Co., Ltd., Tokyo, Japan, yoshiaki.kageji@ss.pacific.co.jp
[7]Tokyo Electric Power Services Co., Ltd., Tokyo, Japan, etamari@tepsco.co.jp
[8]Tokyo Electric Power Services Co., Ltd., Tokyo, Japan, hyoudou@tepsco.co.jp
[9]Jishin Kogaku Kenkyusyo, Inc., Tokyo, Japan, nakama@flush.co.jp
[10]Jishin Kogaku Kenkyusyo, Inc., Tokyo, Japan, atsushi.hosoo@flush.co.jp
[11]Hiroshima University, Hiroshima, Japan, ichiikoji@hiroshima-u.ac.jp

Liquefaction Damage in Urayasu Site

Widespread liquefaction damage occurred at reclaim land in Urayasu city by the main shock (M=9.0) and after shock (M=7.7) of the 2011 off the Pacific Coast of Tohoku Earthquake. The areas focused in this study are shown in Figure 1. “Area 1” is the area with large liquefaction damage as shown in Picture 1, and “Area 2” is the non-damaged area. The settlement after the earthquake in Area 1 was 20 – 30 cm, and settlement was hardly observed in Area 2. The landfill in Area 1 is newer than Area 2.

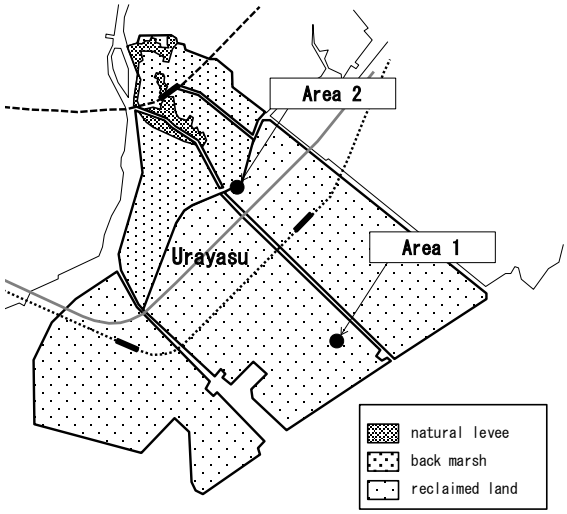

Figure 1: Analysis area

Picture 1: Liquefaction damage at Area 1

Analysis Conditions

An effective stress analysis program “FLIP rose (Iai et al, 1992, 2011)” with the “Cocktail glass model (Iai et al, 2011)” is used for analysis.

Ground Model

The ground model is shown in Figure 2. The ground model is developed as a 1D finite element mesh. The pore water elements were also considered in the shallower ground above the ground water level to simulate the rise in water level by the liquefaction. The negative pore water pressure was set at the ground surface to model the hydrostatic pressure in the ground.

Input Motion

The input motion is shown in Figure 3. Main shock was recorded at Yumenoshima site and after shock was recorded at Urayasu site of K-NET. The pull-up and pull-back analysis (deconvolution of the input motion at the bedrock) was done by DYNEQ, a 1D earthquake response analysis. Because the main shock at Yumenoshima site (5 km east from Urayasu city) was observed at the ground surface and underground deeper than the bedrock and the after shock at Urayasu site of K-NET was only observed at the ground surface.

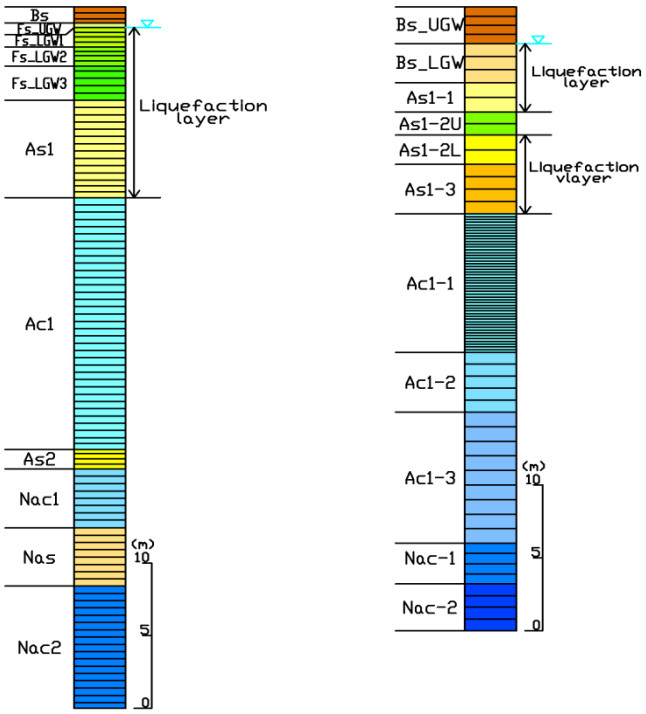

Figure 2: Ground Model

Parameter of the Ground

The parameter of the ground is shown in Table 1. The parameter of the ground is determined from soil property and SPT-*N* value. The parameters for liquefaction property are determined by the simulation of the element test. The liquefaction resistance curves for the parameters determined by the element simulation are shown in Figure 4. The target of the simulation is the liquefaction test result (liquefaction countermeasures and investigation committee in Urayasu city (2012)). The volumetric shrinkage property after liquefaction (Ishihara and Yoshimine (1992)) is also used as the parameter determination.

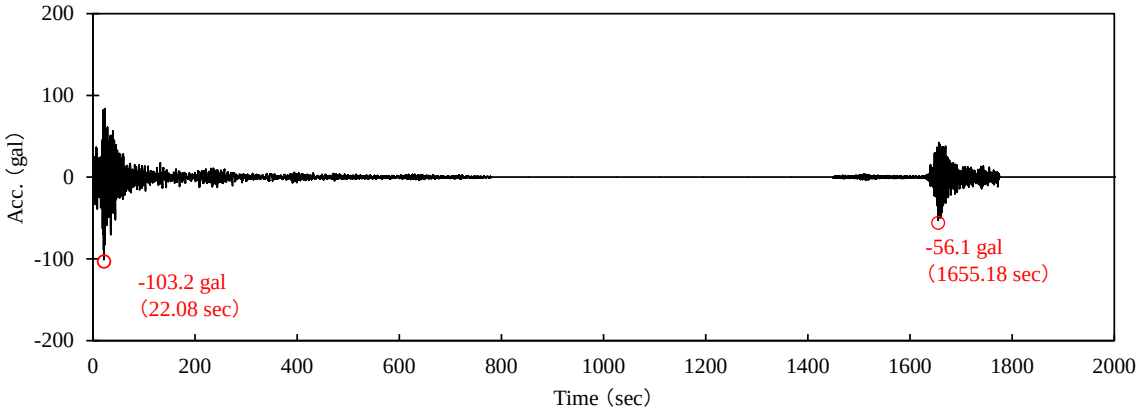

Figure 3: Input motion

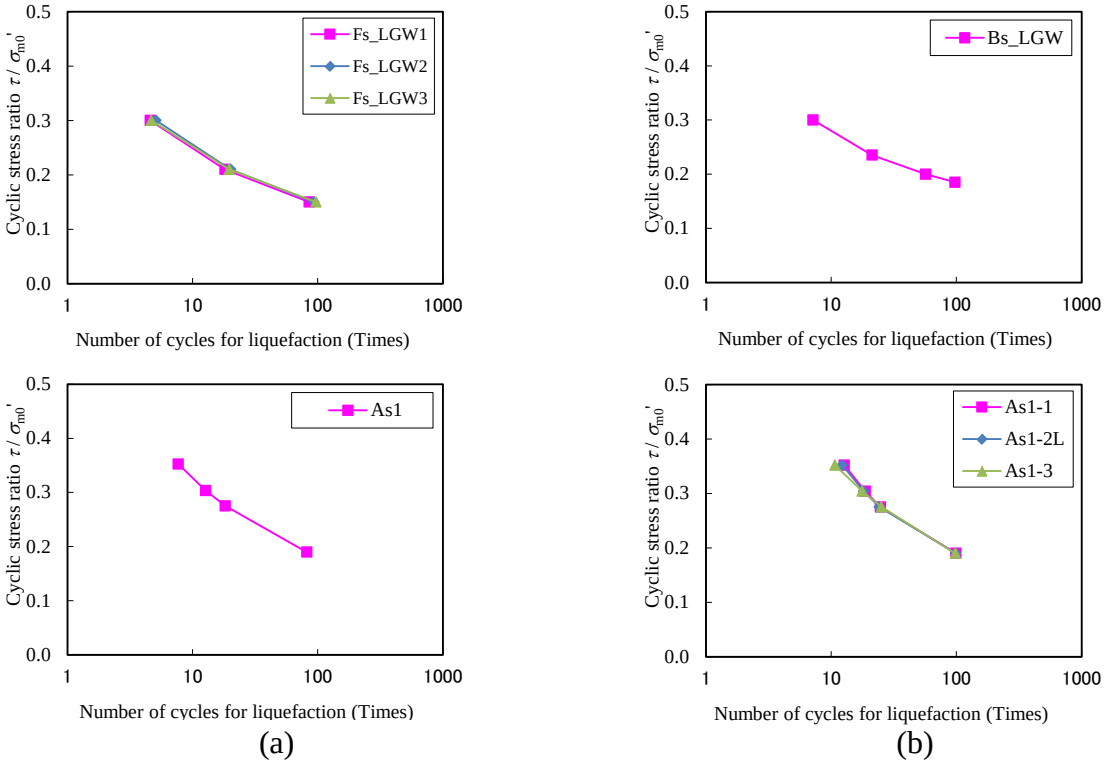

Figure 4: result of the element simulation

Table 1a: Ground parameter at Area 1

Layer	SPT-N value	Density	Reference confining pressure	Elastic shear modulus at a confining pressure	Bulk modulus at a confining pressure	cohesion	Shear resistance angle	Poisson's ratio	Porosity	Maximum damping coefficient	Permeability estimated from D20
	N	ρ (g/cm^3)	σ'_{ma} (kPa)	G_{ma} (kPa)	K_{LA},K_{UA} (kPa)	c (kPa)	ϕ (°)	ν	n	h_{max}	k (m/s)
Bs	---	1.7	98.0	57200	149200	0.0	41.3	0.33	0.45	0.24	5.0E-05
Fs_UGW	10.0	1.8	98.0	40000	104300	0.0	41.0	0.33	0.45	0.24	5.0E-05
Fs_LGW1	10.0	1.8	98.0	34100	88900	0.0	38.3	0.33	0.45	0.24	1.0E-06
Fs_LGW2	3.0	1.8	98.0	32500	87800	0.0	35.6	0.33	0.45	0.24	1.0E-06
Fs_LGW3	0.0	1.8	98.0	25300	66000	0.0	39.6	0.33	0.45	0.24	1.0E-06
As1	8.0	1.8	98.0	34000	88700	0.0	39.4	0.33	0.45	0.24	1.0E-05
Ac1	0.9	1.6	98.0	25600	66800	0.0	30.0	0.33	0.55	0.15	3.0E-08
As2	22.0	1.8	98.0	34900	91000	0.0	40.0	0.33	0.45	0.24	9.0E-06
Nac1	2.5	1.7	98.0	44700	116600	0.0	30.0	0.33	0.55	0.15	3.0E-08
Nas	16.0	1.8	98.0	104000	271200	0.0	39.1	0.33	0.45	0.24	2.0E-05
Nac2	2.5	1.7	98.0	39100	102000	0.0	30.0	0.33	0.55	0.15	3.0E-08

Layer	Phase transformation angle	Parameters for dilatancy											Parameters for volume compressibility		
	ϕ_p (°)	ε_{dcm}	$r\varepsilon_{dc}$	$r\varepsilon_d$	q_1	q_2	q_4	q_{us}	r_y	$rmtmp$	S_1	c_1	l_k	r_k	r_k"
Fs_LGW1	28.0	0.500	0.958	0.500	1.0	0.5	1.0	0.0	0.2	0.5	0.005	1.52	2.0	0.200	0.200
Fs_LGW2	28.0	0.580	0.720	0.580	1.0	0.5	1.0	0.0	0.2	0.5	0.005	1.52	2.0	0.172	0.172
Fs_LGW3	28.0	0.400	0.958	0.400	1.0	0.5	1.0	0.0	0.2	0.5	0.005	1.52	2.0	0.250	0.250
As1	28.0	1.000	0.500	1.000	6.0	2.1	1.0	0.0	0.2	0.5	0.005	1.60	2.0	0.100	0.100

Table 1b: Ground parameter at Area 2

Layer	SPT N-value	Density	Reference confining pressure	Elastic shear modulus at a confining pressure	Bulk modulus at a confining pressure	cohesion	Shear resistance angle	Poisson's ratio	Porosity	Maximum damping coefficient	Permeability estimated from D20
	N	ρ (g/cm^3)	σ'_{ma} (kPa)	G_{ma} (kPa)	K_{LA},K_{UA} (kPa)	c (kPa)	ϕ (°)	ν	n	h_{max}	k (m/s)
Bs_UGW	4.5	1.7	15.9	44408	115810	0.0	41.3	0.33	0.45	0.24	4.0E-05
Bs_LGW	4.5	1.7	39.0	20990	54738	0.0	41.3	0.33	0.45	0.24	4.0E-05
As1-1	3.5	1.8	52.1	41327	107773	0.0	39.4	0.33	0.45	0.24	9.0E-06
As1-2U	25.0	1.8	62.9	47020	122622	0.0	39.4	0.33	0.45	0.24	9.0E-06
As1-2L	5.0	1.8	73.7	47020	122622	0.0	39.4	0.33	0.45	0.24	9.0E-06
As1-3	8.3	1.8	89.9	22224	57958	0.0	39.4	0.33	0.45	0.24	9.0E-06
Ac1-1	0.0	1.6	121.4	19755	51518	0.0	30.0	0.33	0.55	0.15	3.0E-08
Ac1-2	1.0	1.6	152.0	47184	123048	0.0	30.0	0.33	0.55	0.15	3.0E-08
Ac1-3	0.0	1.6	181.5	32000	83451	0.0	30.0	0.33	0.55	0.15	3.0E-08
Nac-1	2.0	1.7	209.1	39031	101786	0.0	30.0	0.33	0.55	0.15	3.0E-08
Nac-2	6.0	1.7	224.9	56204	146571	0.0	30.0	0.33	0.55	0.15	3.0E-08

Layer	Phase transformation angle	Parameters for dilatancy											Parameters for volume compressibility		
	ϕ_p (°)	ε_{dcm}	$r\varepsilon_{dc}$	$r\varepsilon_d$	q_1	q_2	q_4	q_{us}	r_y	$rmtmp$	S_1	c_1	l_k	r_k	r_k"
Bs_LGW	28.0	0.250	1.000	0.500	5.0	1.1	1.0	0.0	0.2	0.5	0.005	1.95	2.0	0.200	0.200
As1-1	28.0	0.625	0.500	0.625	5.0	1.8	1.0	0.0	0.2	0.5	0.005	1.70	2.0	0.160	0.160
As1-2L	28.0	0.625	0.500	0.625	5.0	1.8	1.0	0.0	0.2	0.5	0.005	1.70	2.0	0.160	0.160
As1-3	28.0	0.588	0.500	0.588	5.0	2.8	1.0	0.0	0.2	0.5	0.005	1.40	2.0	0.170	0.170

Permeability of the Ground

The permeability of the ground was determined by D_{20}, particle size passing 20% of the total mass(Creager (1944)). In addition, the parametric study of permeability is done in this study because the permeability may change by the variation in the soil conditions i.e. increase of effective porosity during liquefaction, variation in the degrees of saturation, occurrence of local crack of the ground and so on. The case of the analysis is shown in Table 2.

Table 2: Case of parametric study

		Permeability of liquefaction layer		
		Estimated value from D20	× 10	× 100
Permeability of non-liquefaction layer	× 1/100	Case 1-5	Case 2-5	Case 3-5
	× 1/10	Case 1-4	Case 2-4	Case 3-4
	Estimated value from D20	Case 1-1	Case 2-1	Case 3-1
	× 10	Case 1-2	Case 2-2	Case 3-2
	× 100	Case 1-3	Case 2-3	Case 3-3

Boundary Condition

The boundary condition was as follows: vertically fixed in the base and horizontally fixed in the side at the initial static analysis and the viscous boundary condition in base and the excess pore water pressure on the ground surface is zero at the dynamic analysis.

Analysis Result

Area 1

The time history of the excess pore water pressure ratio is shown in Figure 5. The excess water pressure ratio is increased and liquefaction is occurred. It agree with the observed fact.

Figure 5 (a) is the result for the cases the permeability of the saturated ground (k_1) is constant, but the permeability of the unsaturated ground (k_2) varied. When k_2 is smaller than k_1, the excess pore water pressure ratio of the top of the liquefiable layer (Fs_LGW1) is larger. In addition, the time of dissipation for water pressure tends to be long when k_2 is small. And this tendency is remarkable when the ratio of k_2 and k_1 is big because the water pressure supplied from the bottom of liquefiable layer (Fs_LGW3 and As1) is bigger than the water pressure dissipated at the top of the liquefiable layer (Fs_LGW1).

Figure 5 (b) is the result for the cases the permeability of the unsaturated ground (k_2) is constant, but the permeability of the saturated ground (k_1) varied. When, k_2 is bigger than k_1, the difference of the maximum value of the excess pore water pressure ratio is small. And the time of dissipation for water pressure tends to be long when k_1 is small.

The settlement after liquefaction is shown in Table 3. The settlement after liquefaction is around 20 cm in each case, and it agrees with the observed settlement.

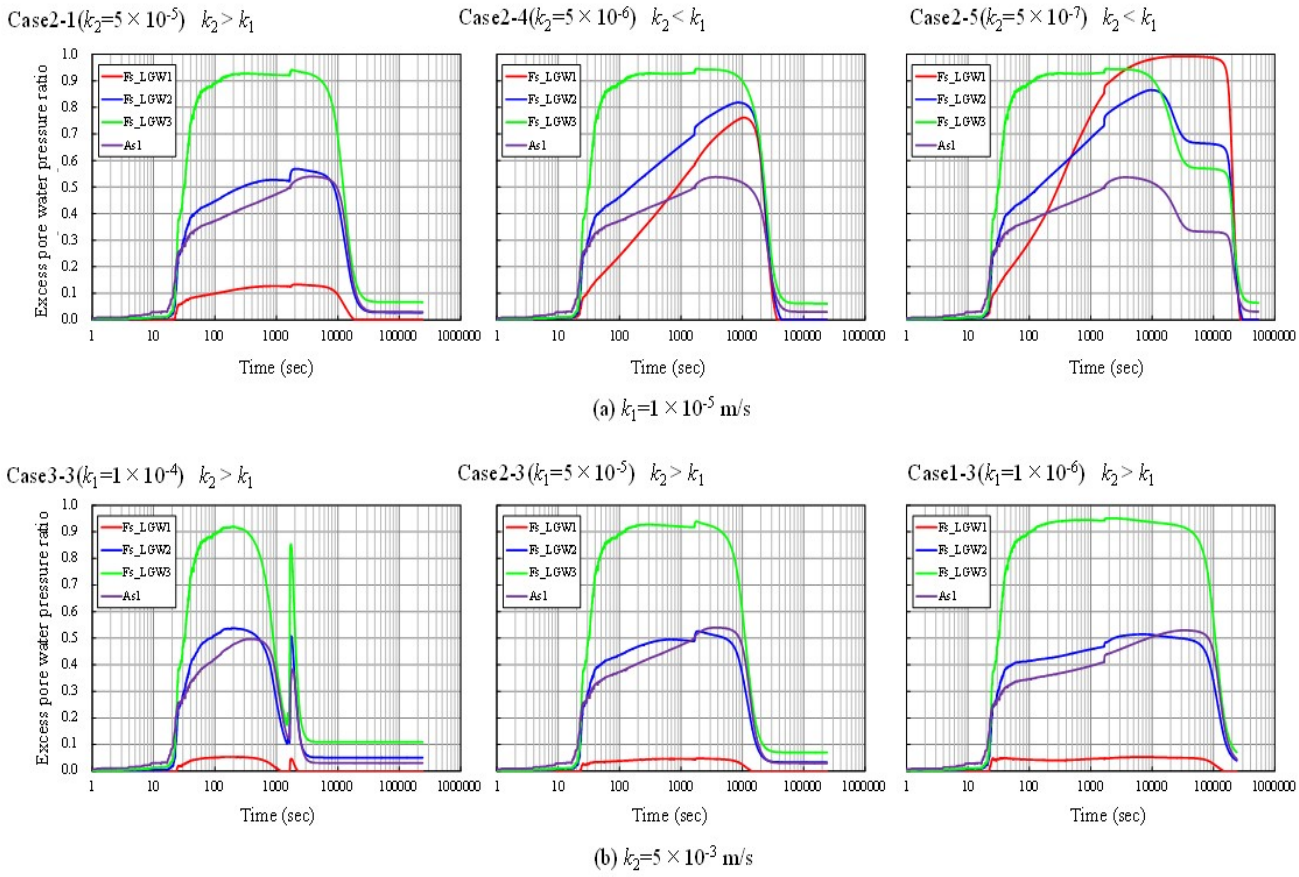

Figure 5. Time history of pore water pressure ratio (Area 1)

Table 3: Settlement after liquefaction (Area 1)

		Permeability of liquefaction layer		
		Estimated value from D20	× 10	× 100
Permeability of non-liquefaction layer	× 1/100	(Case 1-5) 18.4cm	(Case 2-5) 19.8cm	(Case 3-5) 22.4cm
	× 1/10	(Case 1-4) 18.0cm	(Case 2-4) 19.1cm	(Case 3-4) 22.4cm
	Estimated value from D20	(Case 1-1) 18.0cm	(Case 2-1) 18.7cm	(Case 3-1) 21.8cm
	× 10	(Case 1-2) 18.0cm	(Case 2-2) 18.7cm	(Case 3-2) 21.5cm
	× 100	(Case 1-3) 18.0cm	(Case 2-3) 18.7cm	(Case 3-3) 21.3cm

Area 2

Table 4: Settlement after liquefaction (Area 2)

		Permeability of liquefaction layer		
		Estimated value from D20	× 10	× 100
Permeability of non-liquefaction layer	× 1/100	(Case 1-5) 0.8cm	(Case 2-5) 0.9cm	(Case 3-5) 0.9cm
	× 1/10	(Case 1-4) 0.2cm	(Case 2-4) 0.2cm	(Case 3-4) 0.2cm
	Estimated value from D20	(Case 1-1) 1.3cm	(Case 2-1) 1.5cm	(Case 3-1) 1.5cm
	× 10	(Case 1-2) 1.3cm	(Case 2-2) 1.6cm	(Case 3-2) 1.7cm
	× 100	(Case 1-3) 1.4cm	(Case 2-3) 1.6cm	(Case 3-3) 2.1cm

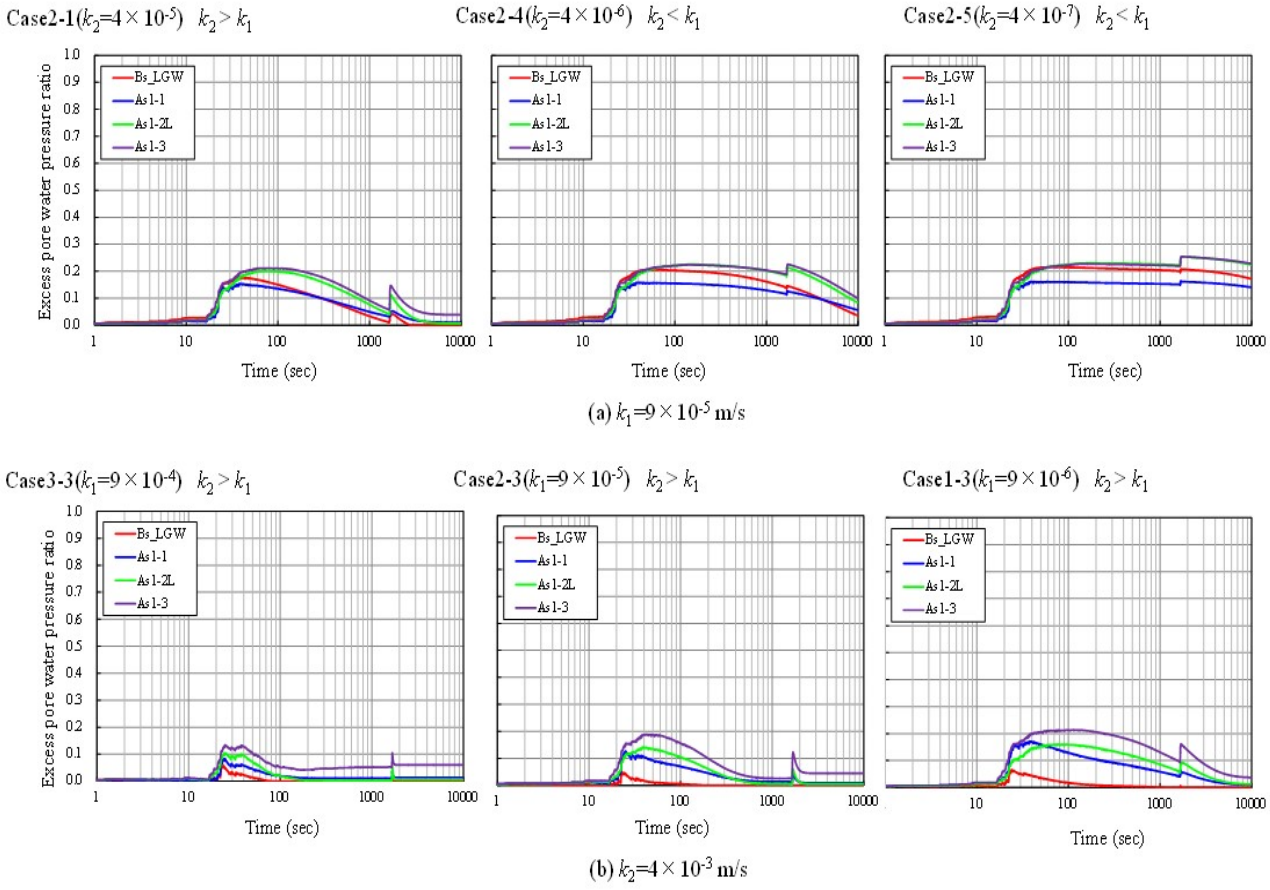

Figure 6 .Time history of pore water pressure ratio (Area 2)

The time history of the excess pore water pressure ratio is shown in Figure 6. The maximum excess water pressure ratio is around 0.2 and liquefaction is not occurred.

The settlement after liquefaction is shown in Table 4. The settlement after liquefaction is smaller than 2 cm in each case, and it agrees with the observation.

Study for Sand Boiling at Area1

The sand boiling was caused by the earthquake at Area 1. Here, a study for sand boiling is done focusing the relationship between the overburden pressure and pore water pressure during the liquefaction at the ground water level.

The pore water pressure generated in the bottom of the non-liquefaction layer W shall be compared with the weight of the non-liquefaction layer G. Then, the sand boiling shall occur when W/G equal to 1.0.

The time histories of W/G in Case1-5, Case2-5, Case3-5 are shown in Figure 7. The permeability of the non-liquefaction layer k_2 of the figure is 1/100 of the estimated value from D_{20}.

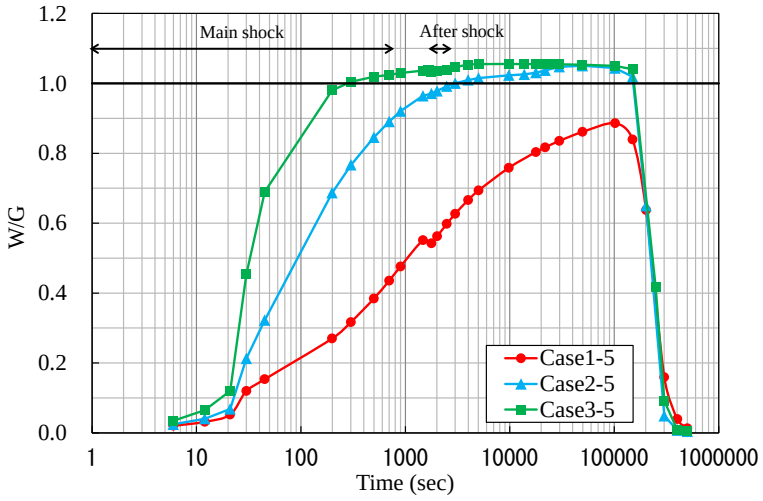

Figure 7. Time history of W/G

According to the record of the security camera nearby the Area 1, the sand boiling is occurred between the main shock and aftershock. W/G in Case2-5 agrees with this observation since it reached to 1.0 between the main shock and after shock. From this result, the permeability of the liquefaction layer may be bigger than estimated permeability from D_{20}. In addition, the sand boiling may be simulated by the appropriate consideration in the permeability of unsaturated ground that is smaller than the permeability in the saturated ground.

Conclusions

In this study, a series of effective stress dynamic analyses considering permeability is done for the areas with and without liquefaction damage at reclaimed land in Urayasu city. The following conclusions were obtained:

1) The applicability of the “Cocktail glass model” to simulate both the the areas with and without liquefaction damage were confirmed.
2) The permeability of the liquefaction layer may be bigger than the estimated permeability from D_{20}. Otherwise, the observed timing of the sand boiling at the site cannot be explained.

Acknowledgements

A series of study in this paper was carried out in the activity of workshop on “FLIP consortium”, Japan. The observed acceleration time history by seismography was opened data through the web site by Tokyo metropolitan government and National Research Institute for Earth Science and Disaster Prevention, Japan. The authors deeply express their gratitude to all the members and related organizations.

References

Iai, Matsunaga, Kameoka. Strain Space Plasticity Model for Cyclic Mobility. *Soils and Foundations*, 1992; **32**(2):1-15.

Iai, Tobita, Ozutsumi, Ueda. Dilatancy of Granular Materials in Strain Space Multiple Mechanism Model. *Int. J. Numel. Meth. Geomech*. 2011; **35**: 360-392.

Ishihara, Yoshimine. Evaluation of Settlements in Sand Deposits Following Liquefaction during Earthquakes. *Soils and Foundations.* 1992; **32**(1):173-188.

Liquefaction countermeasures and investigation committee in Urayasu. Report of liquefaction countermeasures and investigation committee in Urayasu (in Japanese).

National Research Institute for Earth Science and Disaster Prevention Kyoshin Net (K-net). http://www.kyoushin.bosai.go.jp/kyoshin/.

Tokyo Metropolitan Government Bureau of Port and Harbor. http://www.kouwan.metro.tokyo.jp/business/kisojoho/jishindou.html.

Yoshida, S. *DYNEQ:Earthquake response analysis program of the horizontal bedding ground based on the equivalent linear law*. Report of research inst.of Sato Kogyo 61-70. 1996.